THIS PUBLICATION IS DISTRIBUTED TO MEMBERS ONLY

Harmonics and Transients Tech Notes

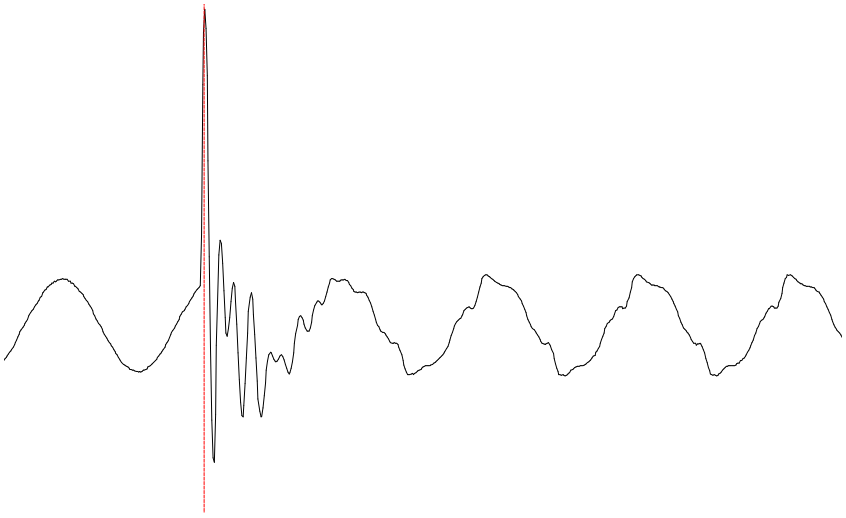

Issue # 96-2 June 1996 Editor: Karen Brown
Project Manager: Susie Brockman
Advisor: Thomas Grebe

In this issue:

Letter from the Project Manager:

Thank you for your support of the Tech Notes and for providing us with quality articles to share. I'd like to briefly update you on a few topics relating to the group.

Users Group Meeting and Workshop

If you have not completed your registration form, but plan to attend, please give me a call so I can add you to the list. If you have a presentation you would like to give at the meeting, please let me know that as well. We already have several signed up, and space is limited, so it is advisable to get your name on the list early. The user's group meeting is an excellent time to interact with other power engineers and exchange ideas about solving power quality problems.

Feedback

This is your user's group and we want to provide you with the tools and support that will make your job easier and also provide a good value for your company. With many utilities cutting back their budgets we want to remain in a price range that will allow you to participate. I would like to get a feeling from you about what services you feel are most worthwhile. If we are failing to provide what you need, I would like to hear from you.

Web Site

Work on the Members Only site is still under construction. You will receive a mailing in a few weeks listing the URL for the site and each member will be given a User ID and password to use. If your account is not current, you will not be able to log on. The latest upgrades of all the user's group software will be available for downloading at your convenience. The internet has introduced a communication tool for today's busy lifestyle. No longer will you be confined by regular business hours for retrieving information.

If you have any questions regarding your membership, please give me a call at (423) 470-9222 ext. 141.

Sincerely,

Susie Brockman
susieb@electrotek.com

For more information concerning the newsletter or to submit a contribution please contact:

Karen Brown
Electrotek Concepts, Inc.
408 North Cedar Bluff Road, Suite 500
Knoxville, Tennessee 37923
Phone: (423) 470-9222 x143 FAX: (423) 470-9223
e-mail: karenb@electrotek.com

A Comprehensive Harmonic Study of Electronic Ballasts and Their Effect on a Utility's 12kV, 10 MVA Feeder

Background

Non-compact or standard ballasts are largely found in industrial areas as well as office buildings, hospitals and libraries. Their primary use is to illuminate large areas. From a utility perspective, the lighting load (kVA) on a specific distribution feeder is due mostly to these non-compact ballasts. Because of this, it is important for a utility to determine the effect on a feeder if energy-efficient electronic ballasts replaced all magnetic ballasts.

Studies have been done in the past on compact fluorescent ballasts including their thermal efficiency [1], their effect on voltage distortion [2] and the effect of undervoltage on their performance [3]. This article builds upon these past studies and goes beyond them [4]. It includes the results of the three stages of research performed on non-compact electronic ballasts for T8 lamps: 1f and 3f laboratory experiments, field testing of buildings selected by Florida Power Corporation (FPC), and computer simulations of a real life FPC 3.6 mile, 12 kV, 10 MVA, 23-bus feeder.

Electronic Ballasts

There are five elements which compose the electronic ballast.

1. Electromagnetic interference (EMI) filter
2. Full bridge diode rectifier, changes incoming ac voltage to dc voltage
3. DC link, usually consisting of a large storage capacitor
4. High-frequency inverter, produces a high-frequency output in the range of 20 to 60 kHz
5. High-frequency transformer whose output is connected to the fluorescent lamp (Figure 1)

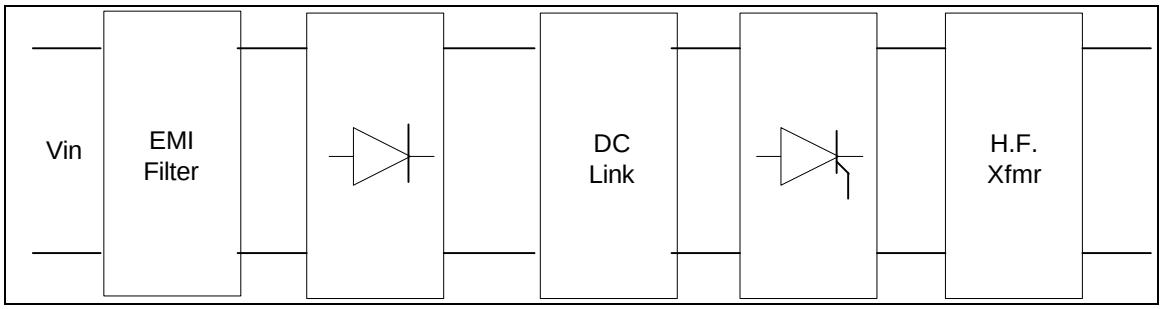

Figure 1: Basic Block Diagram of an Electronic Ballast

Some harmonic distortion will be present in the input current waveform. This is due to the non-linearity inherent in the semiconductor devices used in the electronic ballast.

Recently a "new breed" of electronic ballasts came to the market which exhibit I_{THD}'s below 10%. Some even show I_{THD}'s between 5% to 7%. This may be compared to the "first" generation of electronic ballasts which had I_{THD}'s ranging from 20% to 45%. The electronic ballasts tested in the laboratory displayed an average I_{THD} of 24%.

Research Project Scope

Florida Power Corporation wanted to find answers to the following:

1. What happens to I_{THD} in 1ϕ parallel combinations of: (a) ballasts of the same type, (b) core-coil and electronic ballasts, and (c) "new breed" electronic ballasts?

2. What happens to the neutral current in 3ϕ Y-connected configurations of: (a) core-coil ballasts, (b) electronic ballasts, and (c) "new breed" electronic ballasts?

3. What would happen to the voltage distortion of an FPC building if all the core-coil ballasts were replaced by electronic ballasts?

4. What would happen to the voltage distortion along a real life FPC, 3.6 mile, 12 kV, 10 MVA distribution feeder that has residential, commericial, and industrial loads if all the customers connected to that feeder were to replace all the core-coil ballasts by electronic ballasts?

5. What would be the "maximum allowable" I_{THD} of an electronic ballast that would cause no-change in the existing voltage distortion levels along the same feeder?

Laboratory Experiment Results:

The following are the results of testing performed in three areas: (1) burn-in testing (2) ballasts in 1f parallel combinations and (3) ballasts in 3f configurations.

Burn-In Testing: Twelve four-lamp troffers were tested: four with core-coil ballasts, four with electronic ballasts, and four with "new breed" electronic ballasts, for a 110-hour burn-in period. (ANSI recommends 100 hours), and input measurements (V, I, P, V_{THD}, I_{THD}, etc.) were taken at 25, 50, 75, 100 and 110 hours. Figure 2 shows the I_{THD} versus the time for all twelve four-lamp troffers. The I_{THD} varied: (a) for the core and coil ballasts from 18.32% to 20.36%, (b) for the electronic ballasts from 23.97% to 24.95% and (c) for the "new breed" electronic ballasts from 4.86% to 7.72%. The current waveform and spectrum for the three types of ballasts can be seen in Figure 3.

.

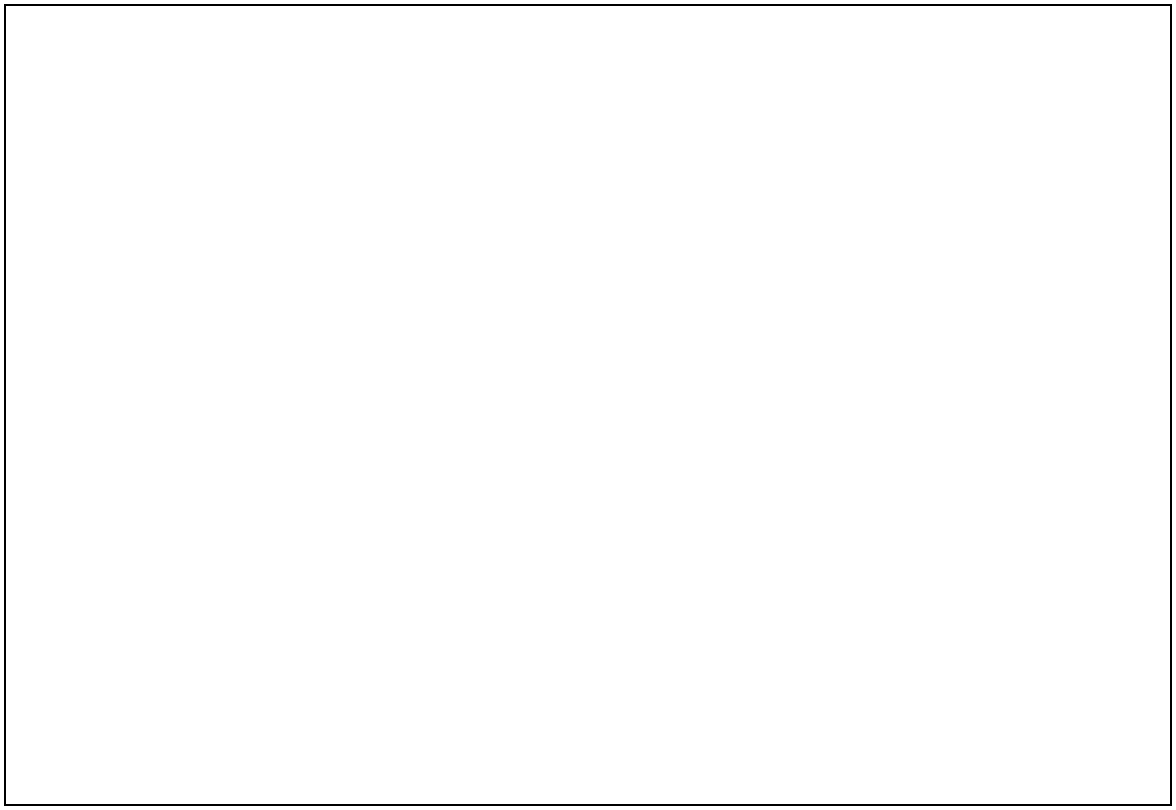

Figure 2: Current for Ballasts vs. Time

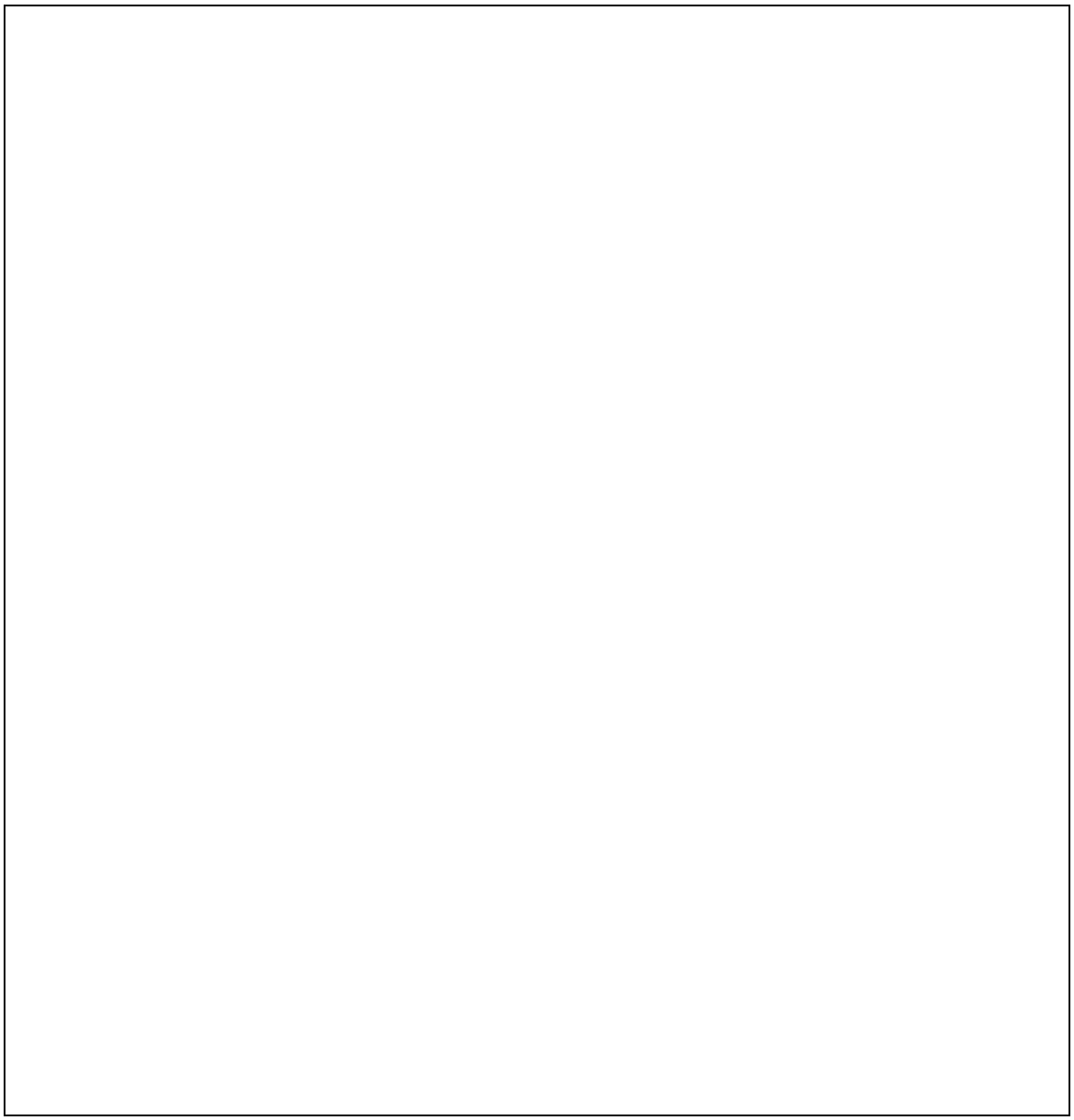

Figure 3: Current Waveforms and Spectra for (from top to bottom) (a) Core-Coil (b) Electronic and (c) "New Breed" Electronic Ballasts

Ballasts in 1f Parallel Combinations. In many facilities, complete ballast retrofits are not always made. This may be for various reasons, but budgetary concerns are often a consideration. It is important to find out what would happen to the I_{THD} if the types of ballasts were to be combined. Figure 4 shows the results.

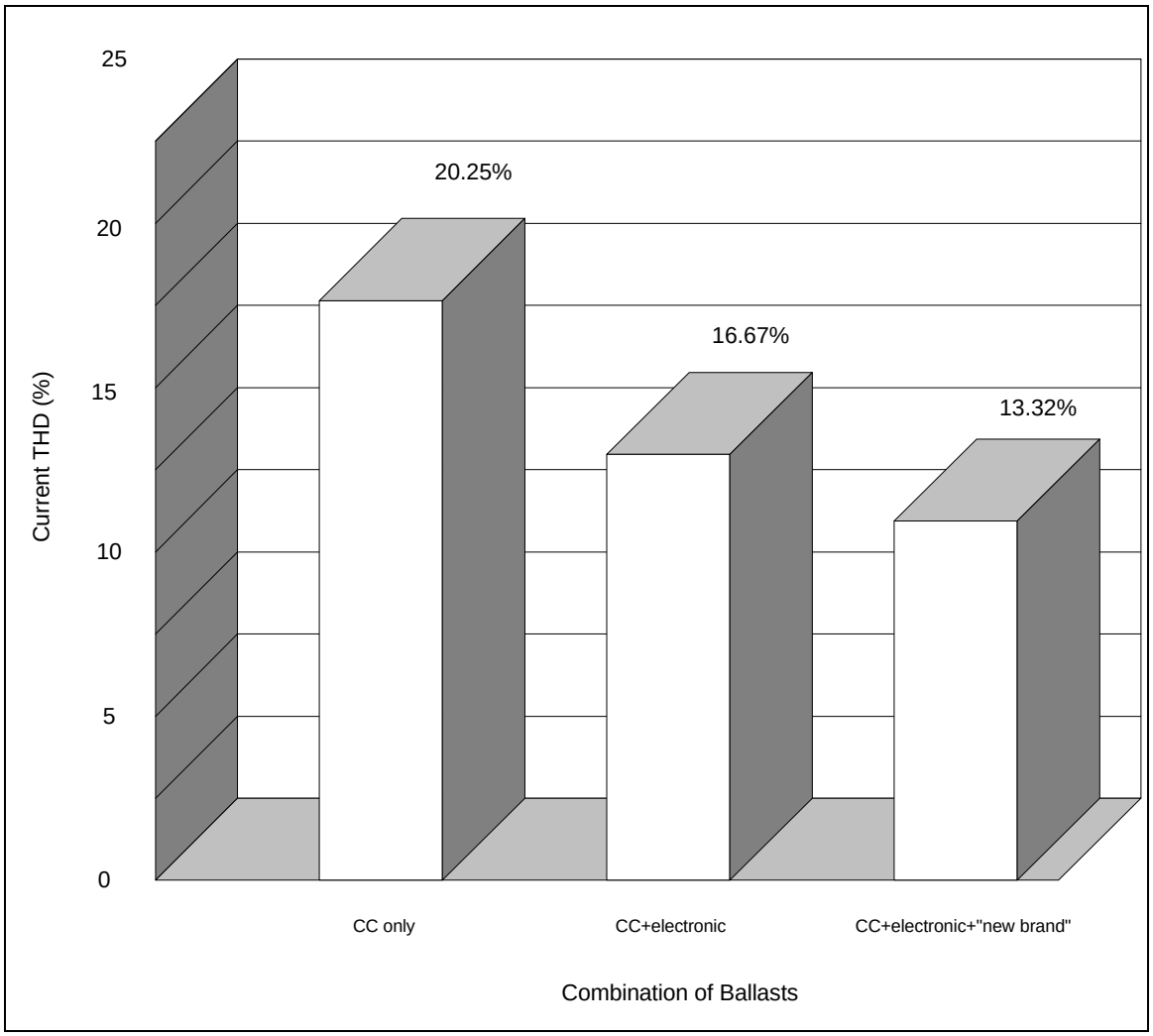

Figure 4: Current THD vs Ballast Combinations

These are the results:

A. When the tested core-coil ballasts were connected in parallel, their I_{THD} remained at about the same level (20%).

B. When the electronic ballasts were added to the core-coil ballasts and the I_{THD} decreased from an average of 20.25% to 16.67%, is interesting since the average I_{THD} for the electronic ballasts (24.4%) was higher than that of the core-coil ballasts (19.48%).

C. When the "new breed" electronic ballasts were added to the previous combination of four core-coil and four electronic ballasts, the lower current drawn by them helped in the reduction of the I_{THD} even further to 13.32%. From these results it can be concluded that by using a combination of these types of ballasts the lighting I_{THD} levels will most likely be reduced.

Ballasts in 3N Configurations: In three experiments, three 4-lamp troffers were connected in wye, and phase and neutral currents were recorded. Figure 5 shows the current waveforms for the core-coil, electronic and "new breed" electronic ballasts' configurations respectively.

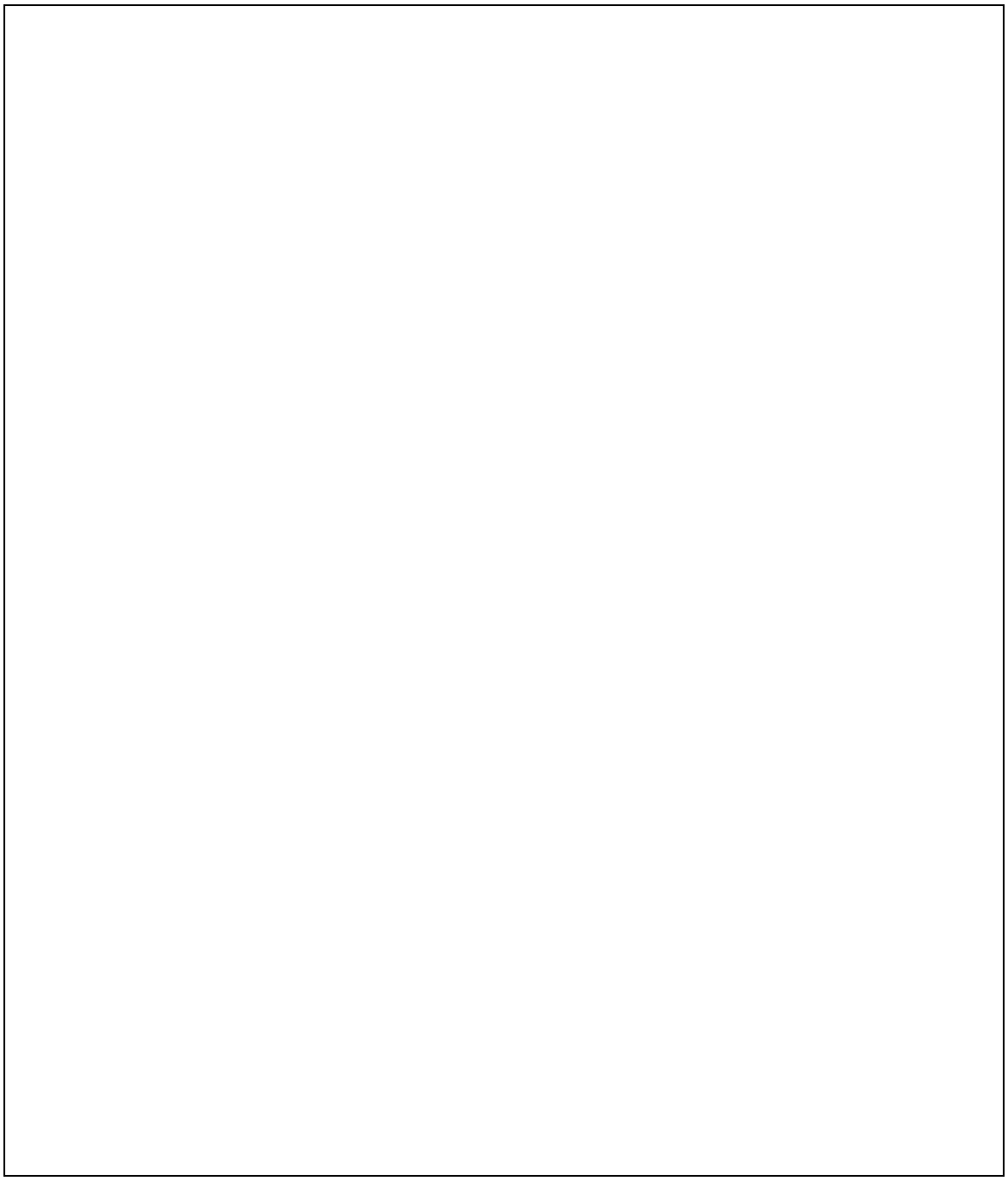

Figure 5: Current Waveforms for 3N Configurations (from top to bottom): for Coil-Core, Electronic and "New Breed" Electronic Ballasts

Table I
Three-Phase Current Measurements for 4-Lamp Troffers
With Different Types of Ballasts

Ballast Type —>	Core-Coil	Electronic	"New Breed"
Avg. I-THD —>	19.48%	24.4%	7.31%
Ia (A)	1.483	0.910	0.896
Ib (A)	1.453	0.906	0.907
Ic (A)	1.479	0.859	0.868
Avg. I rms (A)	1.472	0.892	0.890
Avg. I harm (A)	0.027	0.025	0.002
In (A)*	0.711	0.804	0.127
In (%)**	48.3%	90.1%	14.3%

*Neutral current expressed as a percentage of the average phase current
**I harm = harmonic current only = I fundamental

From Table 1 it is obvious that the "new breed" versus the regular electronic ballasts provided the best scenario with lower phase, neutral and harmonic currents. It is important to note that in "old breed" electronic ballasts the high frequency components in the phase and neutral currents could aggravate interference problems.

Field Testing Measurements

More than seven preliminary field sites were chosen by FPC. After brief testing on all of them, data evaluation and the possibility of follow-up studies on the same sites was performed. This analysis narrowed down the list to three sites upon which to perform more testing.

Before Retrofit Measurements: THD values for voltage and current taken in an office building (site A) during a 35 minute monitoring period showed large standard deviation percentages: 3.76% to 6.03% for voltage, and 20.1% to 32.3% for current. A 24-hour monitoring in another office building (site B) showed the same trend: the maximum V_{THD} never exceeded 2%; however, the I_{THD} average for each phase was about 14% with a high degree of variability.

Figure 6 shows the results of a 41-day monitoring of a building whose load consisted mostly of core-coil ballasts (about 90%), some personal computers and printers. Again, the same trend was found. One of the causes for such large variations in the I_{THD} in the building might be the random and concurrent laser printer activation. When not printing, a particular tested laser printer had 0.63 Arms with an I_{THD} of 170%, and when printing, it had 6.5 Arms with an I_{THD} of 17.6%.

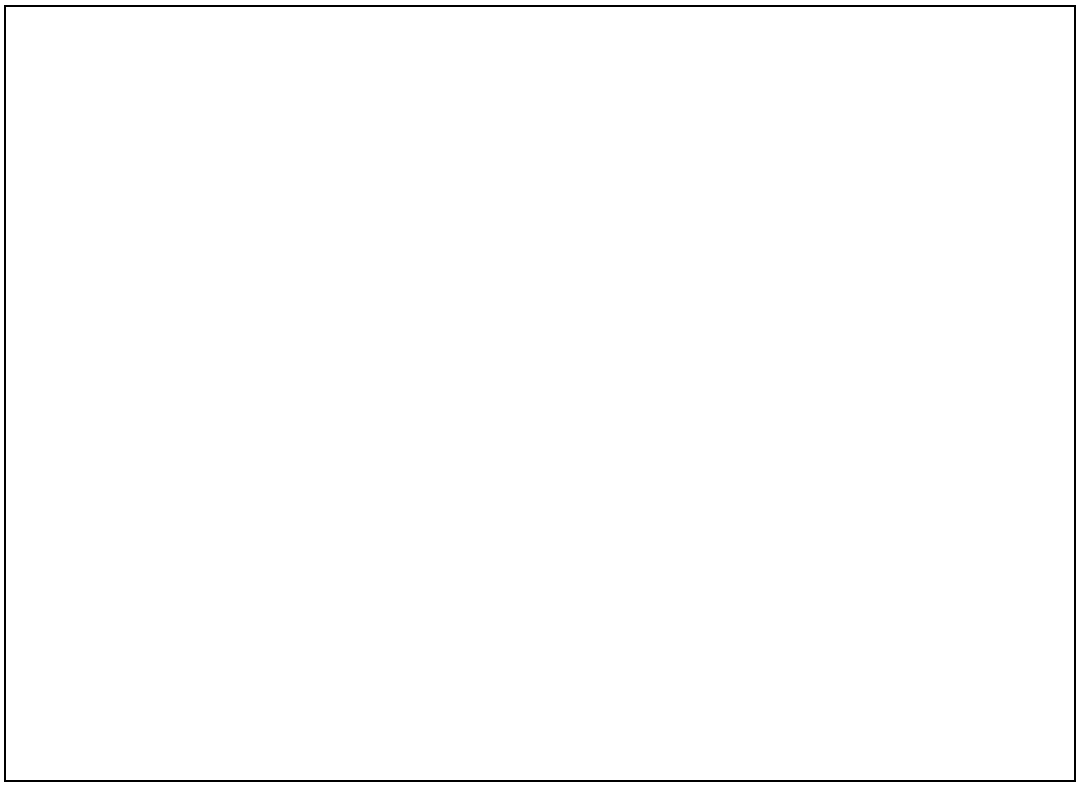

Figure 6: I_{THD} (top) and V_{THD} (bottom) at Site B

After Retrofit: Site C did retrofit its office building with electronic ballasts. Table 2 shows the before and after current values for this site.

Table 2

Table 2: Lighting Load Current in an Office Building (Site C)

Retrofit —>	Before	After	Net Effect
Ia - THD	15.92%	23.50%	Increase
Ib - THD	16.47%	23.27%	Increase
Ic - THD	15.51%	23.55%	Increase
Ia (A)	10.10	7.65	Decrease
Ib (A)	8.38	7.73	Decrease
Ic (A)	9.58	4.86	Decrease
In (A)	3.56	4.02	Increase

As predicted from the laboratory experiments: (a) the I_{THD} increased and the new values were close to the average I_{THD} of 24.4% for the tested electronic ballasts, (b) the current magnitudes decreased and (c) the neutral current did go up for 3.56 to 4.02 A, that is a 12.92% increase which matched very closely to the 13.08%.

Computer Simulations

Computer models and simulations for the core-coil and electronic ballasts, an office building and an actual, 12kV 10MVA feeder were created using a commercially available power system harmonic simulations software package.

Computer Model and Verification for the Core-Coil and Electronic Ballasts, and FPC Building: Both core-coil and electronic ballasts were individually modeled as non-linear current sources, which included harmonic current waveform information up to the 50th harmonic (per IEEE-519-1992); thus, the computer-output current plots for these ballasts reflect this analysis.

To model the FPC office building, a field survey of installed load was taken. The building's field data was also analyzed. The building load consisted mainly of linear load, motors, lighting, and switching mode power supplies. Since the main focus of the harmonic computer simulations was about the "worst" effects of the electronic ballasts, maximum I_{THD} values were used for the core-coil and electronic ballasts. The values obtained from the computer simulations of the FPC building were slightly higher than the field-recorded measurements, on a per-bus basis.

The increase in the predicted value comes from the use of just one computer model for all the ballasts in the building. In reality, the actual ballasts in the building will have some differences in the actual current magnitude and I_{THD} values, which may cause some harmonic cancellation and show up as a lower-magnitude neutral current.

As a result of the analysis on field measurements and the computer model of this FPC building, a computer model was developed to represent the commercial load in the FPC feeder. There were four load types in this model and they had the following load percentage distributions: 24% linear, 41% motors, 5% switching mode power supplies, and 30% fluorescent lighting.

Computer Model and Verification for the 12-kV, 10 MVA Feeder: The actual feeder is a 12.47 kV, 10 MVA feeder with a main radial distance of 3.6 miles, with 23 buses, and three capacitor banks. The load along the feeder is residential, commercial and industrial.

The feeder was modeled using actual FPC data (a) distribution lines with positive, negative, and zero sequence parameters for the cables, (b) three-phase capacitor banks, (c) load-between-switches report for the seven load buses, and (d) field testing and monitoring along seven buses in the feeder. The load types involved in the model were: linear, motor, fluorescent lighting, and switching mode power supplies. Table 3 shows the load type and distribution of the seven buses which were monitored.

Table 3
FPC Feeder Load Type and Distribution

Bus #	Type[a]	kVA	Motor	Linear	Fl[b]	SMPS
3	R	1598.3	45%	45%	3%	7%
7	C	1238.3	41%	24%	30%	5%
9	C	1987.1	41%	24%	30%	5%
12	R	770.4	45%	45%	3%	7%
14	C	216	41%	24%	30%	5%
19	R	216	45%	45%	3%	7%
23	I	3801.4	70%	13%	15%	2%

[a]R* = Residential, C = Commercial, and I = Industrial
b Fl = Non-compact electronic fluorescent lighting

Harmonic Computer Simulations for the Feeder Before and After the Retrofit: Computer simulations were run on this feeder for four cases: before and after the electronic-ballast retrofit for light-load condition (defined by the FPC as 20% of the heavy-load kVA with mostly fluorescent lighting and linear loads), and for the heavy load condition.

From the harmonic simulations run on this feeder (see Figure 7) voltage distortions were obtained only on the buses of interest.

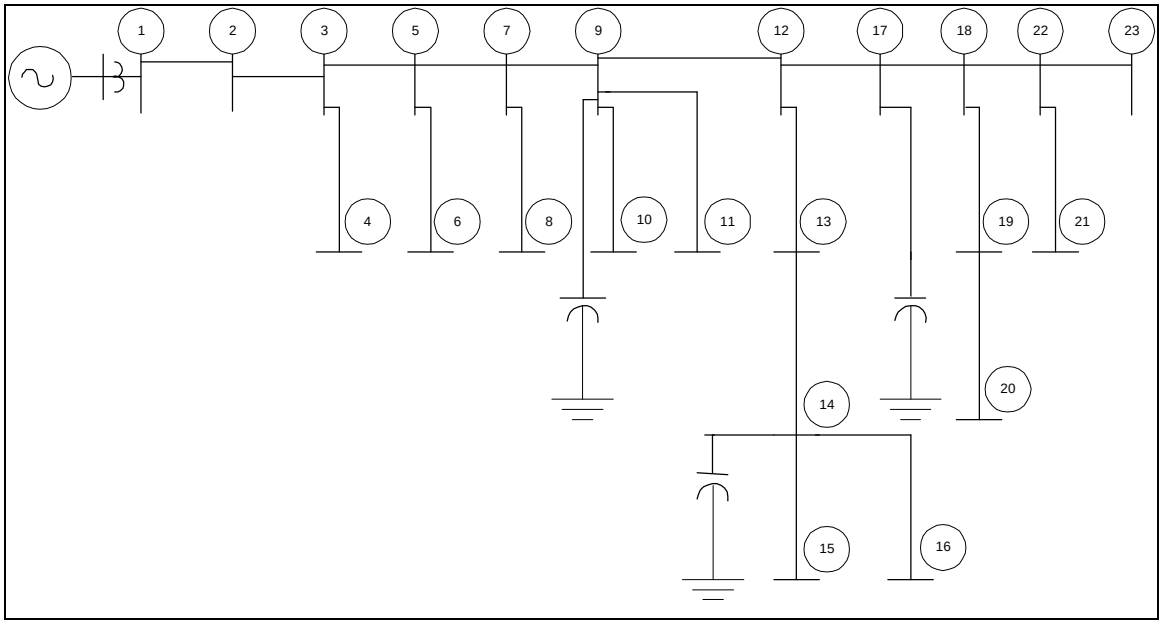

Figure 7: FPC Feeder (12 kV, 10 MVA)

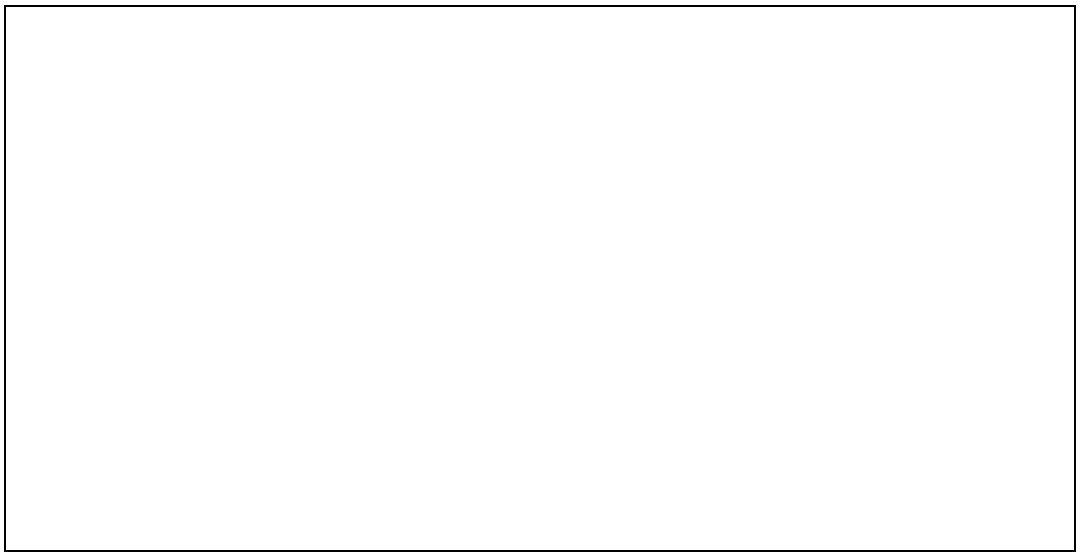

Figure 8: Feeder V_{THD}'s Before and After Retrofit

Note that there was a V_{THD} reduction under both light- and heavy-load conditions after the retrofit with electronic ballasts. The V_{THD} reduction was greater during the light-load condition mainly because the load was made up mostly of fluorescent lighting. Actual field measurements have shown on different occasions V_{THD}'s as high as 8% on bus 23.

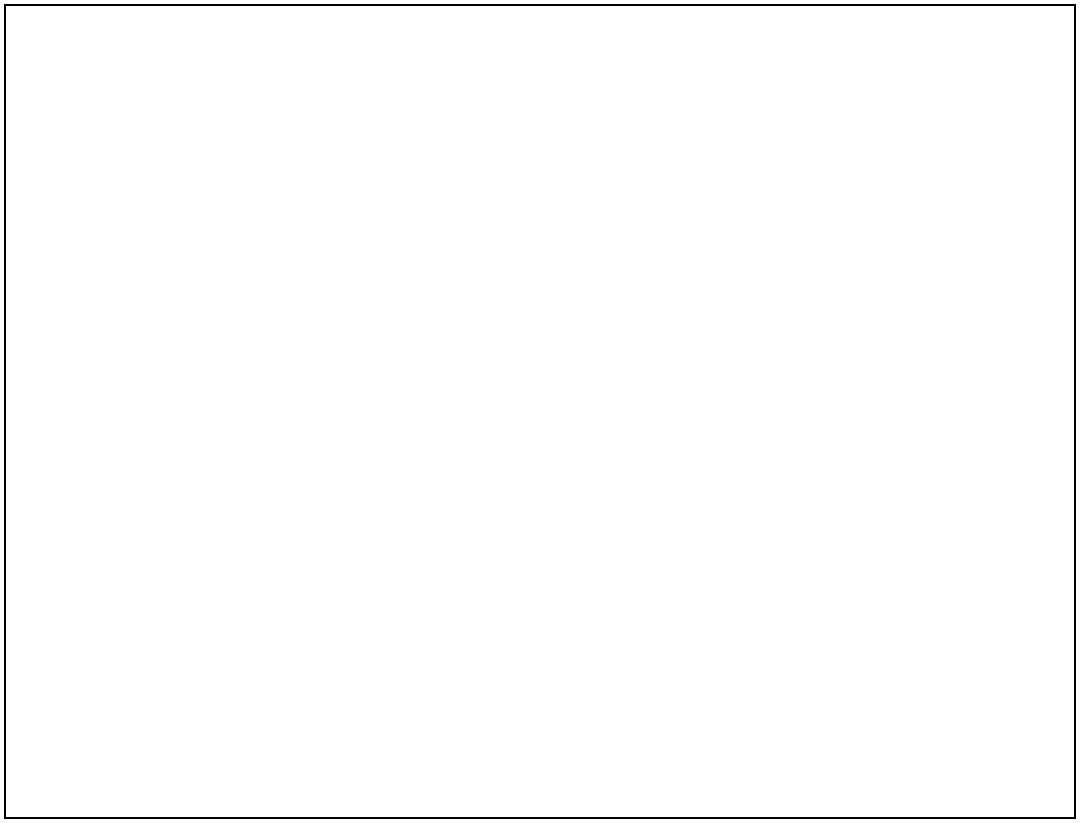

Figure 9: Frequency Scan from Bus 23

A frequency scan was run from the industrial load bus 23, which accounted for 38.7% of the total load. Figure 9 shows the scan at buses 03 and 23 and clearly indicated three resonant frequencies at 340, 1840 and 2750 Hz. Resonant frequency of 340 Hz may account for some of the high V_{THD} values found along that feeder.

Thus as far as the V_{THD} is concerned, this specific feeder would benefit from the electronic ballast retrofit. Next, the utility needed to know what the maximum I_{THD} would be allowed for the electronic ballasts that are going to be used for retrofits, if such ballasts provided the same energy savings.

Computer Simulations to Find Maximum I_{THD} for the Electronic Ballasts: Using the same computer model for the electronic ballasts, its I_{THD} was increased step-by-step and new computer simulations were run each time in order to obtain about the same V_{THD} values that existed along the feeder when core-coil ballasts were used. The goal of the simulations was to find out what the maximum I_{THD} would be for the same energy-efficient ballast if the V_{THD} along the feeder were to remain the same. Ultimately the authors developed an Easy to Comprehend and Assess (ECA) plot (Figure 10) to quickly decide, based upon the I_{THD} and the VA of the ballast, if such a ballast is unacceptable or acceptable.

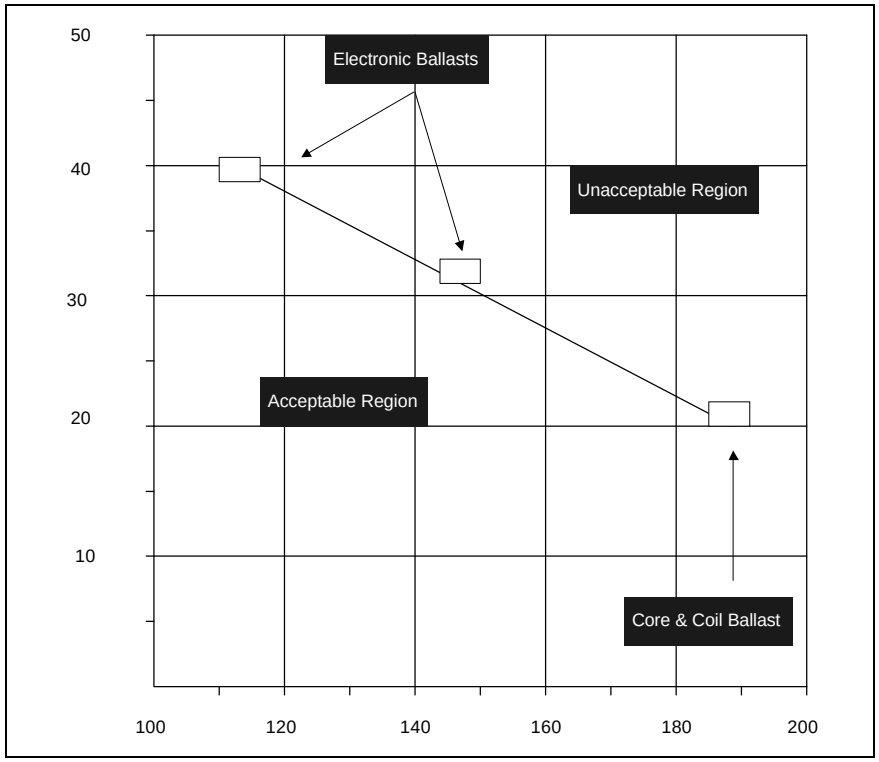

Figure 10: ECA Plot for Electronic Ballasts

Conclusions

These results provided the following answers to the five specific and previously defined questions.

1. When the same type of core-coil ballasts were used in parallel, their I_{THD} remained about the same.

2. When core-coil, and electronic ballasts were combined, harmonic cancellation may have occurred and because of the lower current drawn by the electronic ballasts, the I_{THD} was reduced from 20.25% to 16.67%.

3. When core-coil, electronic and "new breed" electronic ballasts were combined, the 39% lower current drawn by the latter helped in the reduction of the I_{THD} further down to 13.32%.

4. The neutral currents in tested 3f configurations for core-coil, electronic, and "new breed" electronic ballasts were 48.3%, 90.1%, and 14.3% of their phase currents respectively; however, the neutral current increased in the electronic ballasts by 13% and decreased in the "new breed" electronic ballasts by 89% as compared to the core-coil ballast neutral current.

5. The V_{THD} along the FPC 3.6 mile, 12 kV distribution feeder buses was reduced when all the core-coil ballasts were replaced by electronic ballasts. The "maximum allowable" I_{THD} for the particular tested ballast ranged from 40% for a 120-VA ballast to 20% for a 180-VA ballast.

There are numerous types of electronic ballasts with a wide variety of waveforms due to different EMI filter characteristics. The results presented here are for the specific ballasts tested in the laboratory.

References

[1]. M.J. Siminovitch, F.M. Rubinstein, and R.E. Whiteman, "Thermally Efficient Compact Fluorescent Lamps," Proceedings of the IEEE-IAS, Annual Conference, Seattle, WA., Oct. 7-12, 1990.

[2]. D.J. Pileggi, E.M. Gulachenski, C.E. Root, T.J. Gentile, and A.E. Emanuel, "The Effect of Modern Compact Fluorescent Lights on Voltage Distortion," Proceedings of the 1992 IEEE Power Engineering Society Transmission and Distribution Conference, 92SM509-0.

[3]. M.J. Ouellette, and R. Arsenau, "The Effects of Undervoltage on the Performance of Compact Fluorescent Systems," Proceedings of the 1992 Industry Applications Society Annual Meeting, IRC Paper No. 1823, Oct. 1992.

[4]. E. Embriz-Santander, A. Domijan, Jr., and C.W. Williams, Jr., "A Comprehensive Harmonic Study of Electronic Ballasts and Their Effect on a Utility's 12kV, 10 MVA Feeder," IEEE Transactions on Power Delivery, Volume 10, Number 3, July 1995.

E. Embriz-Santander
Florida Power Affiliates
University of Florida
Department of Electrical Engineering

A. Domijan, Jr.
Florida Power Affiliates
University of Florida
Department of Electrical Engineering

C.W. Williams, Jr.
Distribution Engineering
Florida Power Corporation

SuperHarm â Data Preparation

Purpose and Set Up

In order to determine the potential of harmonic voltage and current distortion on a plant distribution system resulting from the installation of adjustable speed GTO Inverter drives for two 8900 horsepower motors, the first step is to build a model of the system. Each drive is a 12 pulse channel made up of two separate six pulse single channel drives. Measurements will be taken on the plant buses during pre-operability testing. This data will then be compared with model data and used to determine the magnitude and effect of induced harmonics on the distribution system.

Modeling Three Phase Systems

Modeling three phase systems is easy using Include (SHI) and Library (SHL) files. Use the main circuit data file (SHA) to reference an Include (SHI) file, which will then reference a Library file (SHL). The resulting parsing file will be identical to files written using only a SHA file.

This example uses the #INCLUDE command to direct SuperHarm® to go to the file listed, library file SYSTEM.SHL, and read the module name, BRANCH. Superharm® will call the SYSTEM.SHL file, and search for the module name BRANCH. SuperHarm®will then pass the parameters listed in parenthesis.

The module name BRANCH can be found in the library file in square brackets, [BRANCH]. In this case the passed parameters are the data required for three-phase branch representation. Each parameter is assigned an identification using %n. The passed parameters are %1 (Name), %2 (From), %3 (To), %4 (R), and %5 (X). For a three phase system the phase representation is added to the NAME, TO (bus) and FROM (bus) by using the "^" symbol following the parameter designation. The " ^" attaches the phase notation to the name, example - NAME=%1^_A.

Using the SHI and SHL files to enter parameters eliminates data entry errors and reduces the size of the circuit data file, SHA. Calling INCLUDE files for major buses makes it easier to debug data files. The data SHI files can be easily added or removed using BLOCK and LINE comments, //, /* info */, or !, to hide the circuit data. Single or multiple library files can be called from the .SHI file.

One final caution - remember all SuperHarm® SHA files must end with an ellipsis - four periods without spaces between the periods. This flags the end of data for the case. This is not an end of file designation and should not be placed at the end of the Include (SHI) or Library (SHL) files.

INPUT FILES USING INCLUDE AND LIBRARY FILES
(Note: Example files do not represent a complete system.)

```
CASE_1.SHA
#INCLUDE 4160_A.SHI
#INCLUDE 4160_B.SHI
....

4160_A.SHI
#LIBRARY SYSTEM.SHL BRANCH (C_P1A, 4100, 4101, 0.0030, 0.0040)
#LIBRARY SYSTEM.AHL 4160LOAD (CP1A, 4101, 1136, 0.900, 0, 0.100)

4160_B.SHI
#LIBRARY SYSTEM.SHL BRANCH (C_P1B, 4200, 4201, 0.0030, 0.0040)
#LIBRARY SYSTEM.AHL 4160LOAD (CP1B, 4201, 1136, 0.900, 0, 0.100)

SYSTEM.SHL
! Library file for passed parameters: subroutine for branch model
! passed parameters:  %1 - Branch Name      %2 - From      %3 - To
!                     %4 - R                %5 - X
[BRANCH]
BRANCH NAME=%1^_A FROM=%2^.A TO=%3^.A R=%4 X=%5
BRANCH NAME=%1^_B FROM=%2^.B TO=%3^.B R=%4 X=%5
BRANCH NAME=%1^_C FROM=%2^.C TO=%3^.C R=%4 X=%5

! subroutine for load model - 4160V
! passed parameters:  %1 - Load Name        %2 - From      %3 - KVA
!                     %4 - DF               %5 - %Parallel  %6 - %Series (motor)
[4160LOAD]
LINEARLOAD  NAME=%1     KV=4.0              BUS.A=%2^.A BUS.B=%2^.B
        BUS.C=%2^.C
KVA=%3      DF=%4       XRCONSTANT=NO           %Parallel=%5  %Series=%6
```

INPUT FILE WITHOUT USING INCLUDE AND LIBRARY FILES

```
CASE_2.SHA
BRANCH NAME= C_P1A _A FROM=4100.A TO=4101.A R=0.0030 X=0.0040
BRANCH NAME= C_P1A _B FROM=4100.B TO=4101.B R=0.0030 X=0.0040
BRANCH NAME= C_P1A _C FROM=4100.C TO=4101.C R=0.0030 X=0.0040

LINEARLOAD   NAME= CP1A   KV=4.0
BUS.A=4101.A BUS.B=4101.B BUS.C=4101.C
KVA=1136              DF=0.900      XRCONSTANT=NO
%Parallel=0           %Series=1.000

BRANCH NAME= C_P1B _A FROM=4200.A TO=4201.A R=0.0030 X=0.0040
BRANCH NAME= C_P1B _B FROM=4200.B TO=4201.B R=0.0030 X=0.0040
BRANCH NAME= C_P1B _C FROM=4200.C TO=4201.C R=0.0030 X=0.0040

LINEARLOAD   NAME= CP1B   KV=4.0
BUS.A=4201.A          BUS.B=4201.B          BUS.C=4201.C
        KVA=1136              DF=0.900      XRCONSTANT=NO
```

Marjorie A. Widmeyer
Washington State University

Application of Distribution System Capacitor Banks and Their Impact on Power Quality

This article presents a summarization of power quality concerns as they relate to the application of distribution capacitor banks.[1] It will discuss the problems associated with distribution capacitor banks, as well as, gives solutions for dealing with these problems.

Introduction

The design of distribution feeders, by necessity, has included the application of distribution system capacitor banks. Other more traditional factors which have also been included are voltage support, power factor and released capacity. Because of its effect on the customer, power quality will become an increasing consideration in this design.

There are two major areas of concern with the application of distribution capacitor banks:

Distribution Capacitor Switching - The frequent switching of distribution capacitor banks coupled with the application of sensitive customer equipment has led to an increased awareness of the magnification of capacitor switching transients and the nuisance tripping of adjustable-speed drives.

Harmonics - Nontraditional customer loads such as adjustable-speed drives are being applied in increasing numbers. These loads often generate excessive harmonic currents that result in unacceptable levels of voltage distortion. Capacitors and the system short circuit impedance combine to create resonances that can magnify harmonic levels to well above acceptable limits.

Distribution Capacitor Switching

Capacitor switching is a normal event on a utility system and the associated transients are generally not a problem. Transients can become a problem if magnification occurs. When this happens, a customer's low voltage power factor correction capacitors are involved.

Problems Associated with Capacitor Switching

Voltage Magnification: Voltage magnification occurs when the transient oscillation, initiated by the energization of the distribution capacitor bank, excites a series resonance formed by the low voltage system. The result is a higher overvoltage at the low voltage bus (Figure 1 [B]). Previous analysis [2] has indicated that the worst magnified transient occurs when the following conditions are met:

- The size of the switched capacitor bank is significantly larger (>10) than the low voltage power factor correction bank (i.e. 3 MVAr vs. 200 kVAr = 15).

- The energizing frequency (f_1) is close to the series resonant frequency formed by the stepdown transformer and the power factor correction capacitor bank (f2) (i.e. f_1 = 490 Hz and f_2 = 670 Hz).

- There is relatively little damping (resistive) provided by the low voltage load (typical industrial plant configuration - primarily motor load).

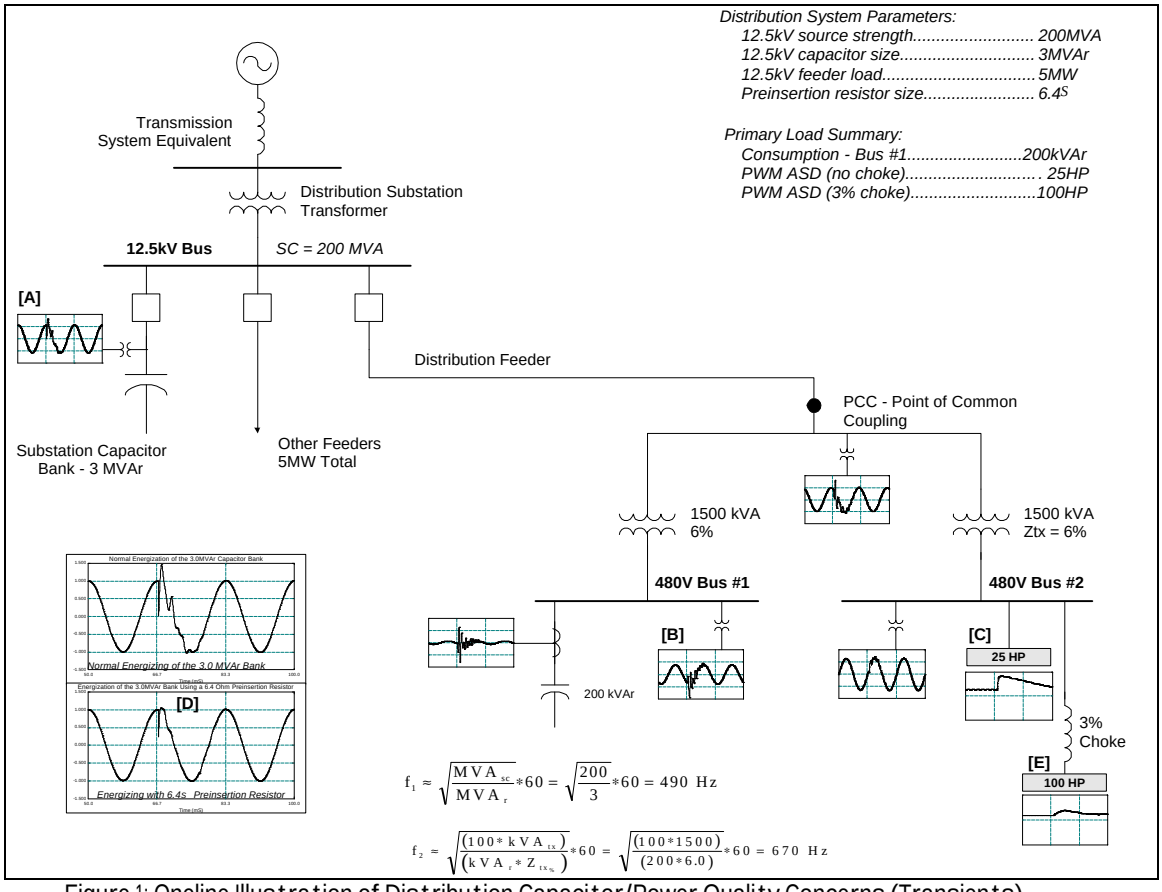

Figure 1: Oneline Illustration of Distribution Capacitor/Power Quality Concerns (Transients)

Computer simulations and in-plant measurements indicate that magnified transients between 2.0 and 4.0 per-unit are possible over a wide range of low voltage capacitor sizes. Customarily, transient overvoltages will damage low-energy protective devices (MOVs) or cause a nuisance trip of a power electronic device. In some cases, however, there has been complete failure of customer equipment.

Nuisance Tripping of Adjustable -Speed Drives: Nuisance tripping refers to the undesired shutdown of an adjustable-speed drive or other power electronic process device due to the transient overvoltage on the dc bus. It is often caused by capacitor bank energization.

The nuisance tripping event consists of an overvoltage trip due to a dc bus overvoltage on voltage-source inverter drives (pulse-width modulated - PWM [3]. Typically, for the protection of the dc capacitor and inverter components, the dc bus voltage is monitored and the drive tripped when it exceeds a preset level. This level is typically around 760 volts (for 480 volt applications), which is only 117% of the nominal dc voltage (Figure 1 [C]). The potential for nuisance tripping is primarily dependent on the switched capacitor bank size, overvoltage controls for the switched bank, the dc bus capacitor size, and the inductance between the two capacitors. Nuisance tripping can occur even if the customer does not have power factor correction capacitors.

Solutions to Capacitor Switching Problems

Identification of the problem is the first step toward a solution. For the most cost effective solution, the customer and utility should work together. The following are some possible solutions:

- The capacitor energizing transient can be controlled using preinsertion resistors/inductors (Figure 2 [D]) or synchronous closing control (technology available for distribution system applications).

- High energy MOV arresters can be applied to the low voltage system. The arresters should limit the overvoltage to approximately 1.8 per unit. The energy rating of the arrester should be evaluated (several thousand joules).

- Harmonic filters can be used for power factor correction. The tuned filter changes the response of the circuit (f_2) and usually reduces the overvoltage level seen at the 480 volt bus. Additional protection can be achieved by placing MOVs across the capacitors.
- Series inductors (chokes) can be installed on the drives to reduce the probability of nuisance tripping. Chokes for this application are commercially available and a size of 3% (of drive rating) is usually sufficient (Figure 2 [E]).

Isolation transformers with similar rating (impedance) will also provide protection.

Harmonics

The voltage signal at any point within a power system is ideally a constant sinusoidal signal which repeats at a rate of precisely 60 times per second, or 60 Hz. Almost all load equipment connected to the electric power system is designed to operate from a sinusoidal voltage source and is said to be linear. That equipment which does not draw sinusoidal current from a sinusoidal voltage source is nonlinear in that the relationship between the voltage and current is not constant every instant of time.

Sources of Harmonics

Those classifications of harmonic sources which present nonlinear voltage/current characteristics to the power system are: saturable devices, arcing devices and power electronics. The nonlinearities resulting from the passive arcing and saturable devices are a result of the characteristics of the electric arc and the iron core. The semiconductor device switching which occurs within a single cycle of the power system fundamental frequency in power electronics equipment is responsible for the nonlinear characteristic.

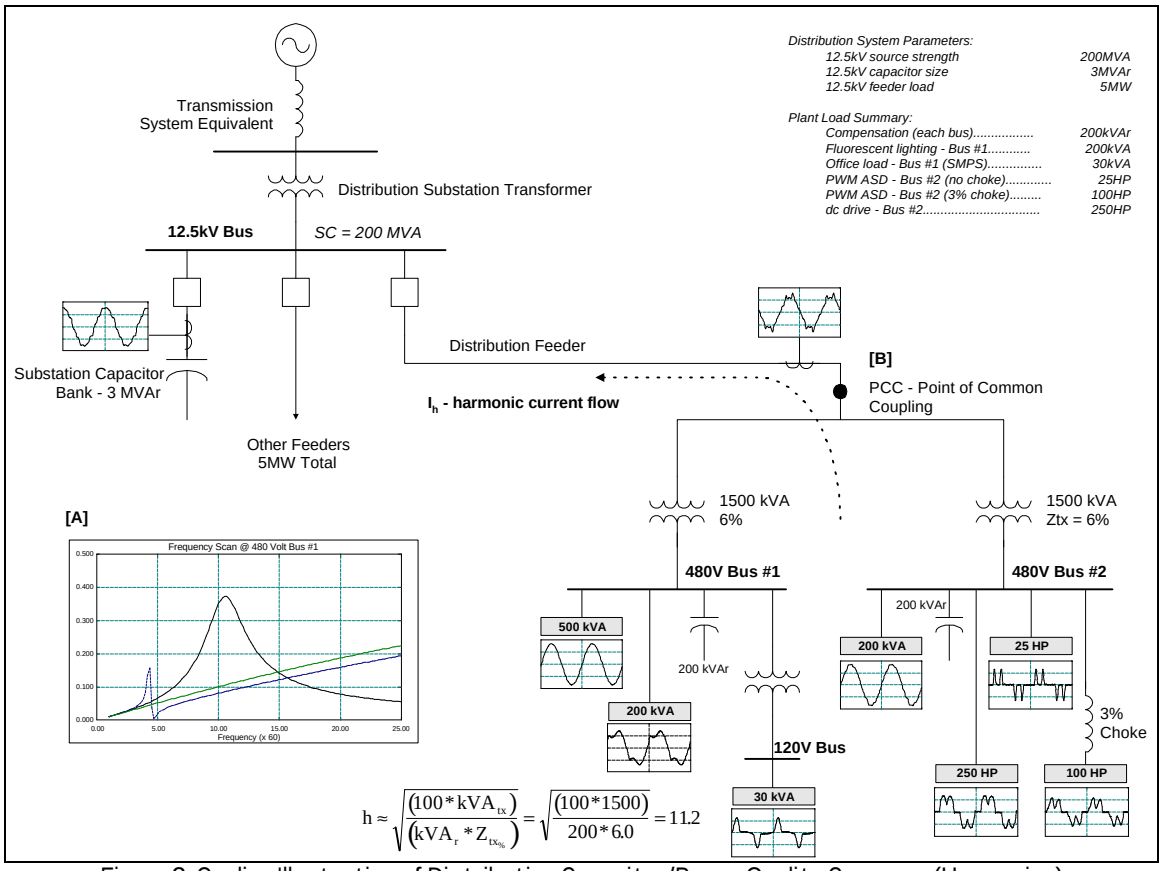

Figure 2: Oneline Illustration of Distribution Capacitor/Power Quality Concerns (Harmonics)

Methods of Harmonic Analysis

Preliminary Assessment: The existence of resonances (high or low impedances) near characteristic harmonic frequencies of loads, identified as harmonic sources, is an indication of potential trouble. Therefore, it is necessary to determine what these system resonant frequencies are. This may be done by using the following equation.

$$h = \frac{1}{2\pi\sqrt{L_{sc}C}} = \sqrt{\frac{X_c}{X_{sc}}} = \sqrt{\frac{MVA_{sc}}{MVA_r}} \approx \sqrt{\frac{(100 * kVA_{tx})}{(kVA_r * Z_{tx\%})}} \qquad \text{(eq 1)}$$

where:

L_{sc} = short-circuit inductance (X_{sc} = reactance)
C = capacitance of bank (X_c = reactance)
MVA_{sc} = short-circuit capacity (3N)
MVA_r/kVAr = stepdown transformer rating (3N)
kVA_{tx} = stepdown transformer rating (3N)
$Z_{tx\%}$ = stepdown transformer impedance

Nearly all harmonic distortion problems occur when this parallel resonance moves close to the fifth or seventh harmonic (h=5 or 7).

Harmonic Measurement: Measurement data validates detailed computer models and hand calculations. The purpose of these measurements is to characterize the behavior of the harmonic sources and to provide preliminary data on the degree of the distortion problem.

Computer Simulation, Calculations: It is necessary to create a representation of the components in a power system and to verify the accuracy of this representation. By doing this, identification of system configurations creating resonances that cause harmonic problems and resonance conditions (Fig.2) can be made.

Solution Development: Harmonic voltage levels determined through both simulation and measurement are evaluated against recommended limits.

Problems Associated With Harmonic Distortion

A principal effect of harmonic distortion is to increase losses and heating in almost every component in the electric power system. While contributing almost no useful work, harmonic components of voltage and current increase the RMS value of voltages and currents. Interaction of harmonic quantities and resistive loss mechanisms in power system components generates excess heat. Some losses are actually sensitive to frequency, so that the power loss per ampere of harmonic current is actually greater than that for fundamental frequency currents. There are several manifestations of those problems associated with harmonic distortion.

- Capacitor banks - usually cause the resonant condition where the highest distortion levels occur.
- Resistive loads - will absorb slightly more power.
- Motor loads - harmonic fluxes within the motor.
- Power transformers - hot spots within the windings.
- Electronic controls - operate improperly.
- Communication circuits - can cause interference.

Apart from the obvious problems stated above, capacitors can make the true power factor worse by creating resonance conditions which magnify the harmonic distortion in the voltage and current.

$$TPF = \frac{Power_{real}}{Voltamperes_{total}} = \frac{P}{V_{rms} * I_{rms}} \qquad \text{(eq. 2)}$$

This is significant because the true power is an indication of the efficiency of energy use. Displacement power factor is very important to most industrial customers because utility billing for power factor penalties is almost universally based on displacement power factor.

$$DPF = Cos\Theta = \frac{kW}{kVA} \qquad \text{(eq. 3)}$$

Solutions to Harmonic Problems

Problems with harmonics often show up at capacitor banks first. The main reason is that capacitors form the resonant circuit that magnifies harmonic current levels causing high voltage distortion levels.

- Apply one single-tuned shunt filter first, designed for the lowest generated harmonic (typically 5^{th}). It is advisable to use capacitors with a higher voltage rating than the system.

- Determine the voltage distortion level at the bus. The commonly applied limit of 5% (total harmonic distortion - THD) was introduces in IEEE Std. 519-1981.

- If required, determine if the harmonic current levels (Figure 3 [B]) meet IEEE Std 519-1992 [4]. If not, there may be a need for multiple filters (i.e. 5^{th} and 7^{th}).

- Vary the filter elements according to the specified tolerances and check its effectiveness.

- Check the frequency response characteristic to verify that the newly created parallel resonance is not close to a generated harmonic frequency (i.e. 7^{th} harmonic filter may create a new 5^{th} harmonic resonance).

Conclusions

- Customer power quality problems can be controlled using a number of different methods.
- Devices being applied to the power system are more susceptible to power quality variations than equipment applied in the past.
- The increasing emphasis on overall power system efficiency is causing a continued growth in the application of shunt capacitor banks.
- Magnification of capacitor switching transients may be the most important concern due to the fact that the transient overvoltages can be very high and the energy levels associated with these transients can cause equipment failure.
- The possibility of nuisance tripping of adjustable-speed drives, due to utility capacitor switching, can be greatly reduced with the application of an input choke.
- Harmonic distortion levels may be reduced with the application of harmonic filters.

References

[1] T.E. Grebe, "Application of Distribution System Capacitor Banks and Their Impact on Power Quality," Presented at 1995 Rural Electric Conference, April 30 - May 2, 1995 Nashville, Tennessee, IEEE #95CH3477-7

[2] M.F. McGranaghan, et al., 'Impact of Utility Switched Capacitors on Customer Systems - Adjustable-Speed Drive Concerns', 1991 IEEE-OES Winter Power Meeting, 91 WM 086-9PWRD.

[3] T.E. Grebe, and L. Tang, "Analysis of Harmonic and Transient Concerns for PWM Adjustable-Speed Drives Using the Electromagnetic Transients Program," Presented at the 5th International Conference on Harmonics in Power Systems, September 23-25, 1992, Atlanta, Georgia.

[4] IEEE Standard 519-1992, 'IEEE Recommended Practices and Requirements for Harmonic Control in Electric Power Systems.

Thomas E. Grebe, PE
Manager, Utility Studies
Electrotek Concepts, Inc.

Single-Phase Nonuniform Transmission Line Model for Tower Representation in Lighting Surge Simulations

Abstract

A nonuniform transmission line model is presented. This model can be used for the representation of transmission towers in lightning surge simulations. The model was recently developed at the University of British Columbia for use with time-domain programs such as the EMTP [1]. It takes into account the nonuniform nature of the tower structure and its associate impedance. Time-domain simulations with the proposed model show good agreement with published experimental results, and with those produced by a cascade multi-section model, where the line is divided into many short sections of uniform transmission lines.

Notation : Uppercase represents frequency domain quantities, whereas lowercase indicates their time domain correspondents.

Introduction

The overvoltage level that lightning can bring about in a power system depends on the surge response characteristics of the object it strikes. The surge response of a transmission tower is not easily understood because, from a wave propagation standpoint, the tower is a non-uniform structure. Its surge impedance is location-dependent and varies as the waves travel through the tower body. Therefore, a nonuniform line model was developed for the purpose of representing the true nonuniform nature of the transmission tower [1]. The parameters of the proposed line model are assumed to vary exponentially. With this assumption, a set of two-port equations can be formed in the frequency domain, which contain frequency-dependent functions. These functions are then synthesized with rational functions of the minimum-phase-shift type. Utilizing a fast recursive convolution technique, the time-domain equations of the proposed model reduce to a form similar to those in Bergeron's method. Thus, the model is compatible with the EMTP. It can be used to faithfully depict the nonuniform nature of the tower structure.

Motivation for Better Tower Models

Many lightning surge simulations using the EMTP often choose to represent the transmission tower as a transmission line with a uniform surge impedance, even though the accuracy of such assumption has not always been verified. This has motivated recent research on more accurate tower models [1-7].

It is relevant to mention that poor lightning performance has been reported on some transmission lines, even if they had very good shielding and low footing resistances [8]. Some lines having low footing resistances have actually displayed outage rates as high as the ones with high values [6]. These unexpected results may well be caused by wave propagation effects up and down the tower. For example, Chisholm [6] pointed out that the influence of the transmission tower on lightning performance may well have been overlooked in many lightning surge simulations. Thus, better tower models are needed.

Previous Tower Models

The transmission tower is a nonuniform transmission line structure, whose surge impedance varies as the surge travels through it. Wagner and Hileman [9] initially derived and proposed a cylindrical tower model with a surge impedance of

$$Z = 60 \ln\left[\sqrt{2}\left(\frac{ct}{r}\right)\right], \qquad \text{(eq. 1)}$$

where t is the travel time counted from the instant the current has entered the tower top, c is the velocity of light and r is the radius of the cylinder.

The equation (1) illustrates that the tower surge impedance is not constant: it is lowest at the top and increases as the wave progresses down to the base. Kawai [10] later performed measurements on isolated towers (without ground wires connected) and obtained a trend similar to the Wagner-Hileman equation, although the magnitudes were appreciably lower. However, the change in the surge impedance in [9] and [10] is opposite to that of most subsequent experiments [11].

Recognizing the inconvenience of the time variation in Eq. (1), Sargent and Darveniza [12] developed a conical tower formula with a uniform surge impedance,

$$Z = 60\ln\left(\frac{\sqrt{2}}{S}\right) \qquad \text{(eq. 2)}$$

where S is the sine of the half angle of the cone.

Chisholm et al [13] later performed experiments as well as analytical calculations, and discovered that the tower surge impedance position-dependent characteristics are dependent upon the direction of the injected current source. To a vertical stroke (current terminating at the tower top), the trend follows that of Kawai's and Wagner-Hileman's results. The trend is opposite for the horizontal situation - where the stroke current terminates somewhere on the ground wire and progresses horizontally as traveling wave towards the tower. To accommodate for the horizontal wave, they devised another equation which characterizes that of an inverted cone,

$$Z = 60\ln\left[\cot\left(\frac{q}{2}\right)\right] \qquad \text{(eq. 3)}$$

where q is the half angle of the cone.

Ishii et al [14] recently performed excellent low current measurements and ascertained that the presence of the connected ground wires alters the change of the measured impedance. Their results confirmed that the surge impedance is higher at the top and lower at the bottom when the tested tower is set up with the ground wires connected to it. These results were used to verify the proposed nonuniform tower model [1].

Exponential Transmission Line Equations

Equations in the Frequency Domain

As indicated in [1], the basic equations for a nonuniform transmission line, expressed in the frequency domain, are

$$-\frac{dV}{dt} = Z(x)I\,, \qquad \text{(eq. 4a)}$$

$$-\frac{dI}{dt} = Y(x)V\,, \qquad \text{(eq. 4b)}$$

V and I are the voltage and current phasors, and Z(x) and Y(x) are the space-dependent per-unit-length series impedance and shunt admittance, respectively.

Differentiating equation (4a) again leads to

$$-\frac{d^2V}{dt^2} = Z(x)\frac{dI}{dx} + \frac{dZ(x)}{dx}I \,. \qquad \text{(eq. 5)}$$

Substituting (4a) and (4b) into (5) gives

$$\frac{d^2V}{dx^2} = Z(x)Y(x)V + \left(\frac{dZ(x)}{dx}\frac{1}{Z(x)}\right)\frac{dV}{dx} \,. \qquad \text{(eq. 6)}$$

For the exponential line shown in Figure 1, with losses ignored, Z(x) and Y(x) are

$$Z(x) = jwL(x) = jwL_0e^{qx}, \qquad \text{(eq. 7a)}$$

$$Y(x) = jwC(x) = jwC_0e^{-qx}, \qquad \text{(eq. 7b)}$$

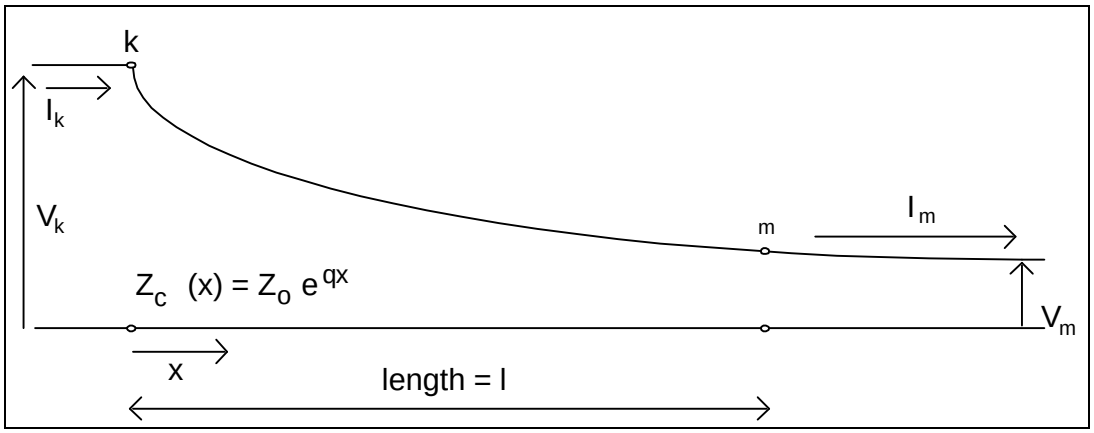

Figure 1: Single Phase Exponential Line

where L(x) and C(x) are the per-unit-length inductance and capacitance, respectively; L_0 and C_0 are the values at x = 0. These parameters are related to the high-frequency approximation of the line characteristic impedance,

$$Z_{high}(x) = \sqrt{\frac{Z(x)}{Y(x)}} = Z_0e^{qx}, \qquad \text{(eq. 8)}$$

where $Z_0 = \sqrt{\frac{L_0}{C_0}}$.

Substituting (7a) and (7b) into (6) gives

$$\frac{d^2V}{dx^2} - q\frac{dV}{dx} - \frac{w^2}{c^2}V = 0 \qquad \text{(eq. 9)}$$

where $c = \frac{1}{\sqrt{L_0 C_0}}$ is the wave speed.

Equation (9) is the second-order differential equation with the roots

$$l_1 = \frac{q}{2} - \sqrt{\left(\frac{q}{2}\right)^2 - \left(\frac{w}{c}\right)^2}; \quad l_2 = \frac{q}{2} + \sqrt{\left(\frac{q}{2}\right)^2 - \left(\frac{w}{c}\right)^2}. \qquad \text{(eq. 10)}$$

Then,

$$V(x) = C_1 e^{l_1 x} + C_2 e^{l_2 x}, \qquad \text{(eq. 11)}$$

and from (4a),

$$I(x) = -\frac{1}{Z(x)}\left[l_1 C_1 e^{l_1 x} + l_2 C_2 e^{l_2 x}\right]. \qquad \text{(eq. 12)}$$

The constants C_1 and C_2 depend on the boundary conditions. As shown in the Appendix A of [1], the voltages and currents at both ends can be related as

$$[V_k + Z_{ck}(w) I_k]A = V_m + Z_{cm}(w) I_m, \qquad \text{(eq. 13)}$$

where $A = e^{l_1 l}$ is the propagation function. Z_{ck} and Z_{cm} are the characteristic impedances at both ends of the line, which (as indicated in the Appendix A of [1]) have the form of

$$Z_{ck}(w) = \frac{jwL_0}{l_2} \quad and \quad Z_{cm}(w) = \frac{jwL_0 e^{ql}}{l_2}. \qquad \text{(eq. 14)}$$

By letting w go to infinity in equation (10) and inserting the result $l_1 = l_2 = \frac{jw}{c}$ into equation (14), the characteristic impedances become the high-frequency approximation of equation (8).

Equations in the Time Domain

Reversing the current direction at node m to make it flow into the line (Figure 1), $I_{mk} = -I_m$, equation (13) in the time domain becomes

$$[v_k(t) + z_{ck}(t)] * a(t) = v_m(t) - z_{cm}(t) * i_{km}(t), \qquad \text{(eq. 15)}$$

where the symbol '$*$' denotes convolutions.

If the characteristic impedances Z_{ck} and Z_{cm}, together with the propagation function A, can be synthesized with rational functions, their corresponding expressions in the time domain will then become simple sums of exponential functions. The function a(t) will also have a time delay, which approximately equals the time it takes for the fastest frequency component to travel the line. Accordingly, the convolutions in equation (15) can be evaluated with a fast recursive algorithm [15]. Thus, the voltage at node m can be expressed in a simpler form as

$$v_m(t) = z_{meq} i_{mk}(t) + v_{hRC_m}(t) + v_{pro_m}(t), \qquad \text{(eq. 16)}$$

where z_{meq} is a constant. The last two terms on the right hand side are evaluated from the known values of previous time steps. The first term comes from the RC-network which approximates the characteristic impedance, and the second term comes from the propagation of conditions at the remote end k. Combining these two terms into a single history voltage source $e_{h\text{-}m}(t)$, equation (16) becomes

$$v_m(t) = z_{meq} i_{mk}(t) + e_{h-m}(t). \qquad \text{(eq. 17)}$$

The same procedure is used to evaluate the voltage at node k, but with the wave direction from node m to node k instead. Factor q has opposite sign now, and the roots in (10) must therefore be re-evaluated. The characteristic impedances and the propagation function of the line are also recalculated, using these new roots. Carrying out the necessary steps, the voltage at node k can then be expressed in the same from as equation (17),

$$v_k(t) = z_{keq} i_{km}(t) + e_{h-k}(t). \qquad \text{(eq. 18)}$$

Equations (17) and (18) are very similar to those in Bergeron's method. They are compatible and can be easily interfaced with the EMTP, with the equivalent of circuit of Figure 2.

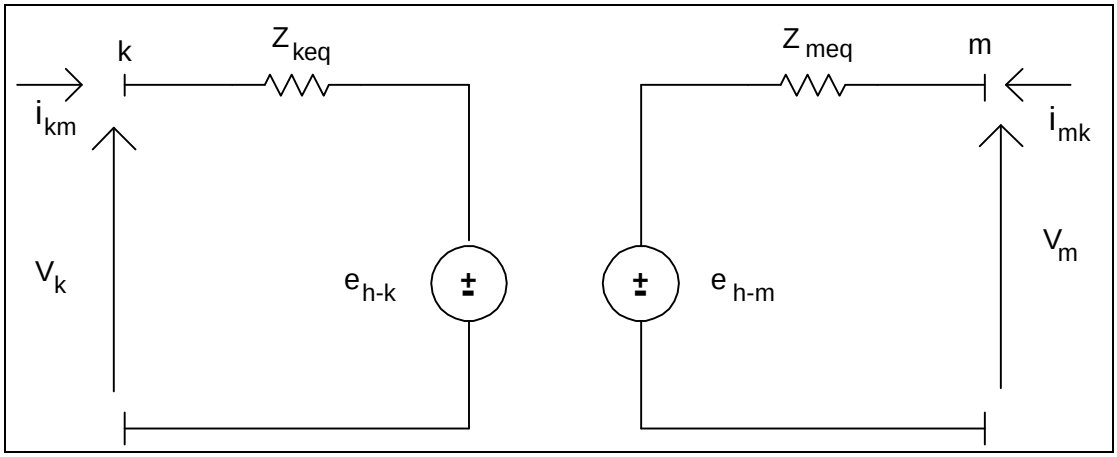

Figure 2: Equivalent Circuit for the Exponential Line

Validity of the Proposed Nonuniform Line Model and EMTP Field Test Comparison

Recursive convolutions leading to equations (17) and (18) are possible only if the line characteristic impedances and propagation function are synthesized successfully. The synthesis results, as shown in [1], were excellent. The line parameters were synthesized using stable minimum-phase rational functions. Open and short circuit simulations in the time domain were performed and the validity of the proposed nonuniform line model was also verified in [1]. These results will not be repeated here. However, it is relevant and useful to present the simulation of the Ishii et al's experiment again.

As mentioned previously, Ishii and his associates made low current measurements on 500 kV double-circuit towers [14]. Their experimental set-up is similar to the case where lightning strikes the transmission towers, except that the current source was low in magnitude. The circuit parameters for EMTP simulation are displayed in Figure 3. The circuit consists of three sections of a double-circuit line with the geometry of Figure 4, of three transmission line towers, and of a low current source with a 400 W source impedance. A 300 m cable with a surge impedance of 50 W is connected between the source and the tower top. All of the conductors are terminated with 350 W resistors at both ends. The rest of the parameters used are similar to those described in [14], with the exception of the line model: the authors of [14] used the Semlyen frequency-dependent model, while

a constant-parameter line model is used here. The difference has no noticeable effect on the insulator voltages in this case. As can be seen in Figure 3, the middle tower No. 7 is modeled as 4 transmission line sections, three uniform and one exponential line, with the crossarms ignored, In concurrence with the measured impedances in [14], the uniform sections have a uniform surge impedance of 220 W, while the exponential one has a nonuniform surge impedance of 220 W at the upper end and 150 W at the bottom end. Capacitances of the insulator strings and stray capacitances from the phase conductors to the tower are also modeled. The simulated and measured waveforms of the three crossarm insulator voltages (potential difference between crossarm and phase conductor) at tower No. 7 are shown in Figure 5. A time delay approximately 1 ms is seen in these voltages because of the connected cable between the current source and the tower top. The voltages are very close compare to the measurements. Thus, the simulation results supports the validity of representing transmission towers with the proposed exponential transmission line model.

It should be mentioned that the capacitances (from the insulator string and from the phase conductor to the tower) influence and retard the electromagnetic field propagation in the transverse direction. This aspect is not taken into account by the conventional time-domain transmission line models because they only represent the TEM mode in the horizontal direction [16] . Without including these capacitances, the lower-phase insulator voltage would have the highest magnitude. This would be the opposite of what had been measured.

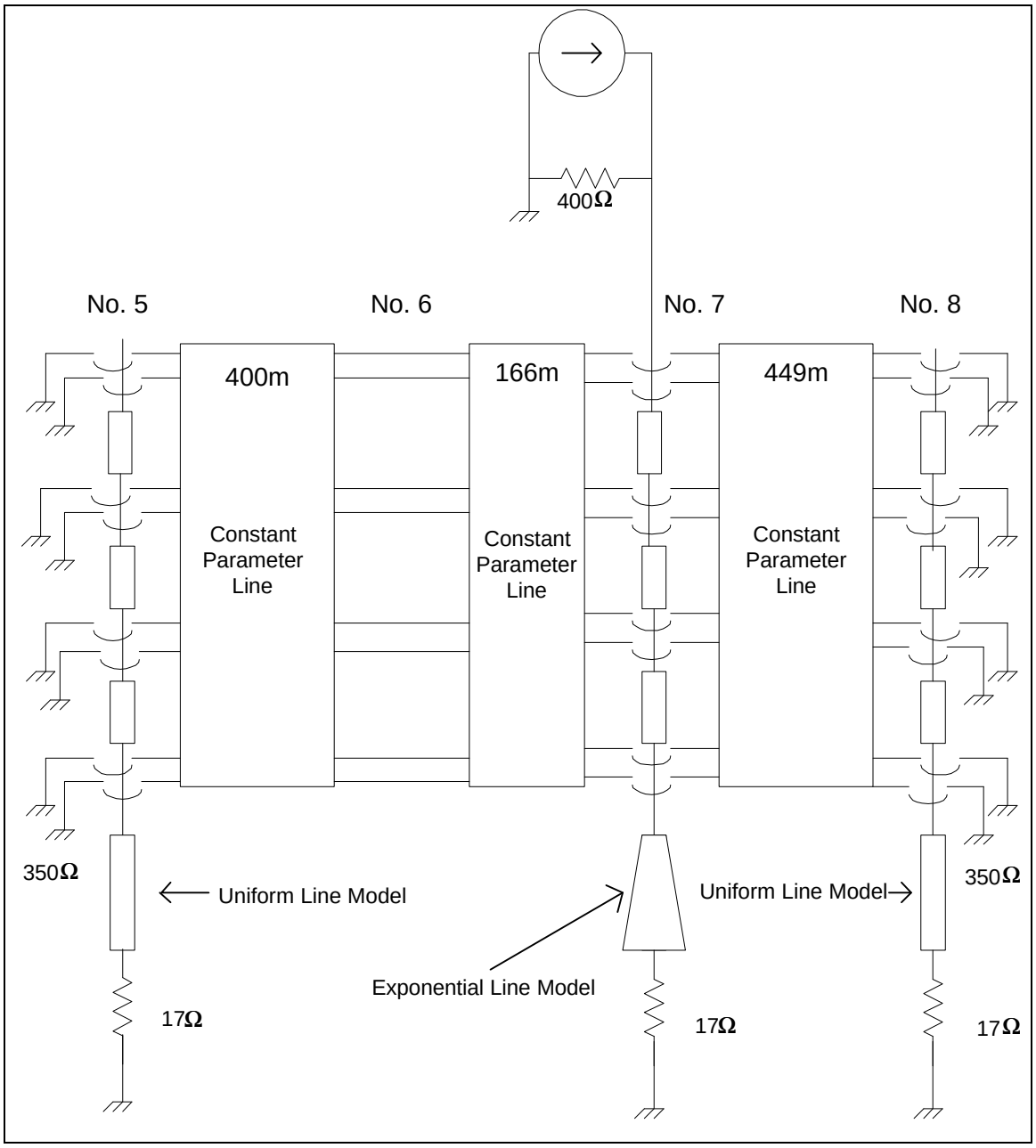

Figure 3: Circuit for the EMTP Simulations

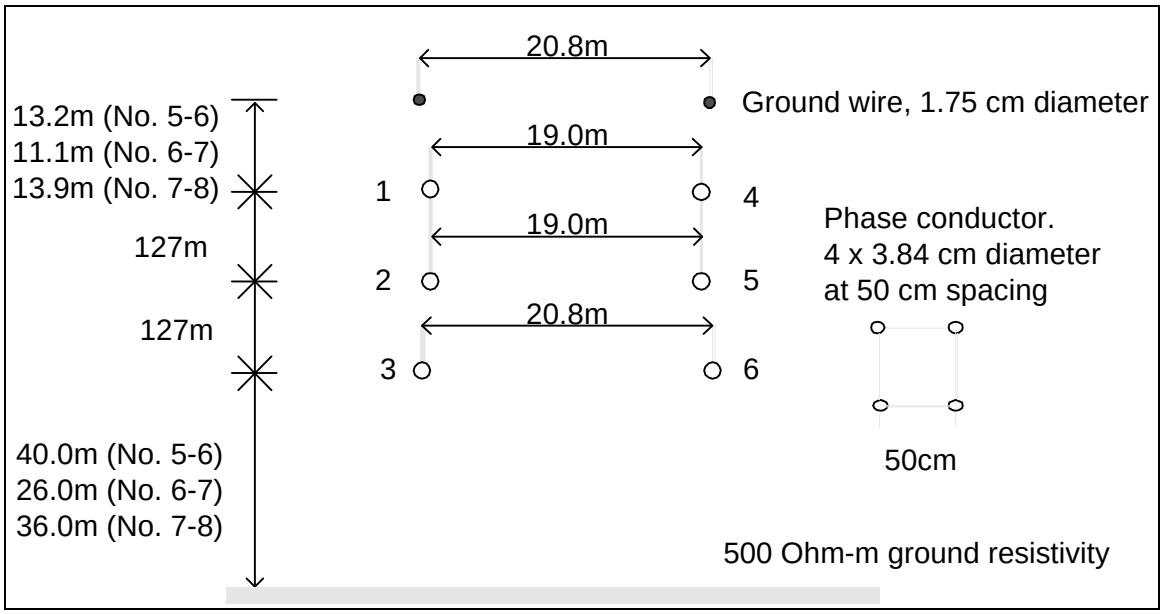

Figure 4: Conductor Geometry at Average Height

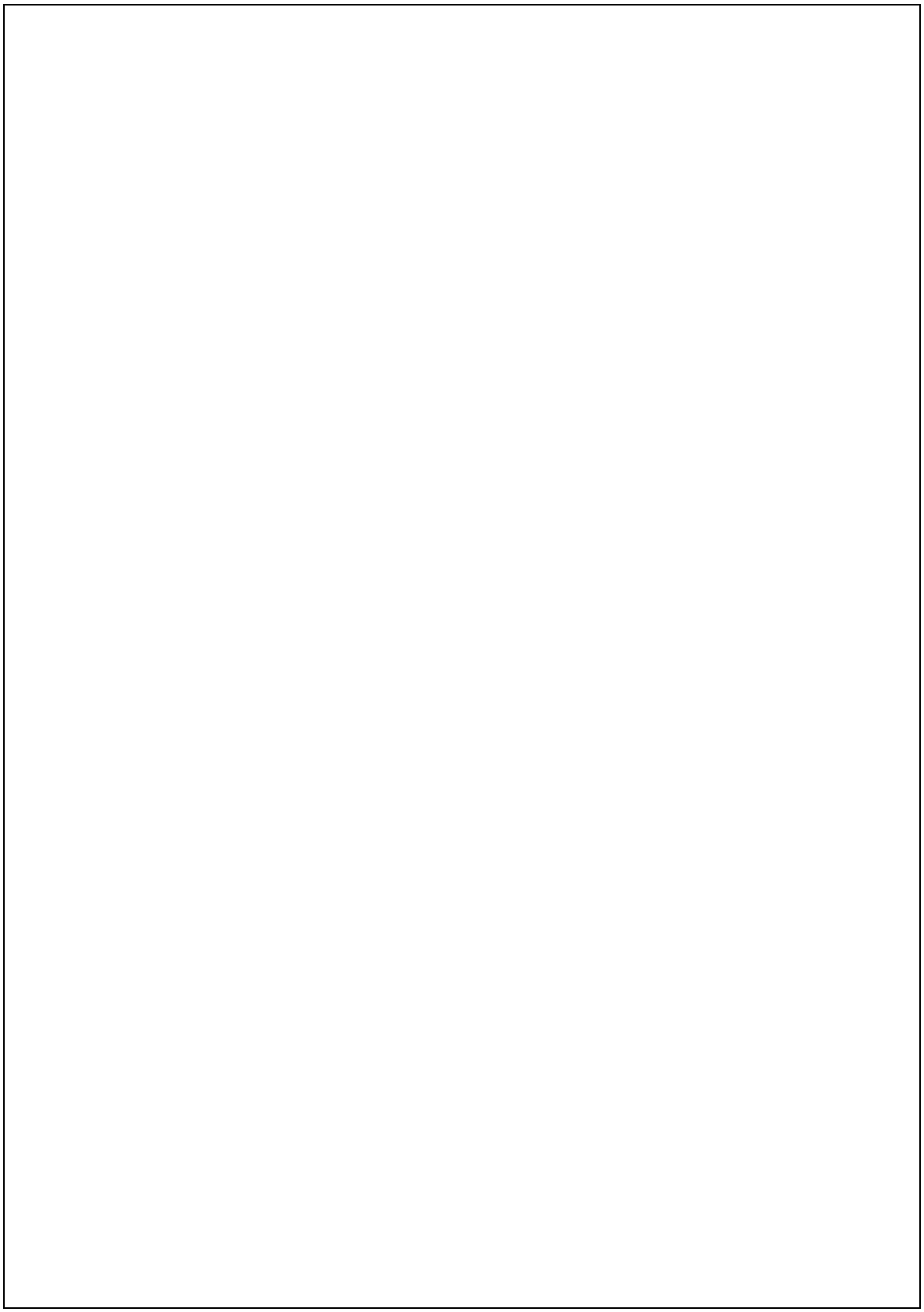

Figure 5: Simulation of Ishii et al experiment and measurement from [14]

Conclusion

An exponential tapered line model has been presented. It is compatible and can be interfaced with the EMTP. The model is numerically stable because it synthesizes the line functions in the frequency domain with stable rational functions of minimum-phase type. Time-domain simulations with the proposed model show good agreement with experimental results from the literature. The model is primarily intended for the representation of the transmission line towers in lightning surge simulations. It can also be used to model general nonuniform lines with complicated space-dependent characteristic impedances, as described in [4].

Acknowledgments

The author would like to thank professors H.W. Dommel and J.R. Marti for their guidance and support in this work.

References

[1] H.V. Nguyen, H.W. Dommel, J.R. Marti, "Modelling of Single-Phase Nonuniform Transmission Lines in Electromagnetic Transient Simulations," IEEE Paper No. 459-8 PWRD, Summer Power Meeting, Denver, Colorado, July 28 - August 1, 1996.

[2] M.T. Correia de Barros, M.E. Almeida, "Computation of Electromagnetic Transients on Nonuniform Transmission Lines," IEEE Paper No. 397-0 PWRD, Summer Power Meeting, Portland, Oregon, July 1995.

[3] H.V. Nguyen, H.W. Dommel, J.R. Marti, "Tower Models for Lightning Surge Simulations," IEEE Paper No. 045-5 PWRD, Winter Power Meeting, New York, New York, Feb. 1994.

[4] E.A. Oufi, A.S. Alfuhaid, M.M. Saied, "Transient Analysis of Lossless Single-Phase Nonuniform Transmission Lines," IEEE Trans. on Power Delivery, Vol. 9, No. 3, pp. 1694-1701, July 1994.

[5] M.M. Said, A.S. Alfuhaid, M.E. Elshandwily, "S-Domain Analysis of Electromagnetic Transients on Nonuniform Lines," IEEE Trans. on Power Delivery, Vol. 5, No. 4, pp. 2072-2083, November 1990.

[6] W.A. Chisholm, "Lightning Surge Response of Transmission Towers and Lines," Ph. D. Thesis, University of Waterloo, Department of Electrical Engineering, 1983.

[7] C. Menemenlis and Z.T. Chun, "Wave Propagation on Nonuniform Lines," IEEE Trans. on Power Apparatus and Systems, Vol. PAS-101, No. 4, pp. 833-839,1982.

[8] J.T. Whitehead, "Lightning Performance of TVA's 161-kV and 500-kV Transmission Lines," IEEE Trans. on Power Apparatus and Systems, Vol. PAS-102, No. 3, pp. 752-768, 1983.

[9] C.F. Wagner and A.R. Hileman, "A new Approach The Calculation of The Lightning Performance of Transmission Lines III-A Simplified Method: Stroke to The Tower," AIEE Trans. on Power Apparatus and Systems, Vol. 79, pp. 589-603, 1960.

[10] M. Kawai, "Studies of The Surge Response of a Transmission Line Tower," IEEE Trans. on Power Apparatus and Systems, Vol. 83, pp 30-34, 1964.

[11] P.G. Buchan and W.A. Chisholm, "Surge Impedance of HV and EHV Transmission Towers," Final Report for Canadian Electrical Association Contract #78-71, 1980.

[12] M.A. Sargent and M. Darveniza, "Tower Surge Impedance," IEEE Trans. on Power Apparatus and Systems, Vol. PAS-88, No. 5, pp. 680-687, 1969.

[13] W.A. Chisholm et al, "Lightning Surge Response of Transmission Towers," IEEE Trans. on Power Apparatus and Systems, Vol. PAS-102, No. 9, pp. 3232-3242, 1983.

[14] M. Ishii et al, "Multistory Transmission Tower for Lightning Surge Analysis," IEEE Trans. on Power Delivery, Vol.6, No.3, pp. 1327-1335, 1991.

[15] J.R. Marti, "Accurate Modeling of Frequency-Dependent Transmission Lines in Electromagnetic Transient Simulations," IEEE Trans. on Power Apparatus and Systems, Vol. PAS-101, pp. 147-157, 1982.

[16] H.V. Nguyen, Discussion of " Computation of Electromagnetic Transients on Nonuniform Transmission Lines," Paper 95 SM 397-0 PWRD, IEEE PES Summer Meeting, Portland, 1995.

Huyen Van Nguyen
Senior Power Systems Engineer
Electrotek Concepts, Inc